GLIA

WILEY

RESEARCH ARTICLE

Sexual dimorphism in the inflammatory response to traumatic brain injury

Sonia Villapol[1] | David J Loane[2] | Mark P Burns[1]

[1]Laboratory for Brain Injury and Dementia, Department of Neuroscience, Georgetown University, Washington, District of Columbia

[2]Department of Anesthesiology, Center for Shock, Trauma, and Anesthesiology Research (STAR), University of Maryland School of Medicine, Baltimore, Maryland

Correspondence
Mark P. Burns, Department of Neuroscience, Georgetown University Medical Center, New Research Building-EG11, 3970 Reservoir Rd, NW, Washington, DC 20057.
Email: mpb37@georgetown.edu

Funding information
NIH grants, Grant numbers: R01NS067417 (M.P. Burns), R01NS082308 (D.J. Loane), and R03NS095038 (S. Villapol)

Abstract

The activation of resident microglial cells, alongside the infiltration of peripheral macrophages, are key neuroinflammatory responses to traumatic brain injury (TBI) that are directly associated with neuronal death. Sexual disparities in response to TBI have been previously reported; however it is unclear whether a sex difference exists in neuroinflammatory progression after TBI. We exposed male and female mice to moderate-to-severe controlled cortical impact injury and studied glial cell activation in the acute and chronic stages of TBI using immunofluorescence and *in situ* hybridization analysis. We found that the sex response was completely divergent up to 7 days postinjury. TBI caused a rapid and pronounced cortical microglia/macrophage activation in male mice with a prominent activated phenotype that produced both pro- (IL-1β and TNFα) and anti-inflammatory (Arg1 and TGFβ) cytokines with a single-phase, sustained peak from 1 to 7 days. In contrast, TBI caused a less robust microglia/macrophage phenotype in females with biphasic pro-inflammatory response peaks at 4 h and 7 days, and a delayed anti-inflammatory mRNA peak at 30 days. We further report that female mice were protected against acute cell loss after TBI, with male mice demonstrating enhanced astrogliosis, neuronal death, and increased lesion volume through 7 days post-TBI. Collectively, these findings indicate that TBI leads to a more aggressive neuroinflammatory profile in male compared with female mice during the acute and subacute phases postinjury. Understanding how sex affects the course of neuroinflammation following brain injury is a vital step toward developing personalized and effective treatments for TBI.

KEYWORDS
cytokine, inflammation, microglia, sex-differences, trauma

1 | INTRODUCTION

The activation of resident microglial cells, alongside the infiltration of peripheral macrophages, are key neuroinflammatory responses to traumatic brain injury (TBI). These inflammatory responses are a classic component of the secondary injury cascade and are associated with neuronal death (Corps, Roth, & McGavern, 2015). This neuroinflammation begins in the acute phase but can last for years postinjury in both humans and animals (Loane et al., 2014; Kumar et al., 2013; Rice et al., 2017; Smith et al., 2013). Microglial/macrophages (MG/Mϕ) are the main players in propagating inflammation to tissues neighboring the core site of injury. They perform this task through the production of inflammatory mediators including cytokines and chemokines. The activation of MG/Mϕ can be observed experimentally by examining time specific changes in morphology, and the production profiles of pro- and anti-inflammatory cytokines, nitric oxide, prostaglandins, or chemokines (Harry & Kraft, 2008; Kettenmann, Hanisch, Noda, & Verkhratsky, 2011; Ransohoff & Perry, 2009).

Microglia are resident immune cells in the brain that are activated in response to injury (Saijo & Glass, 2011). CNS injury also induces macrophage recruitment from the periphery, whose role is to rapidly access the injury site as a first line of defense against infection (Corps et al., 2015; Mishra, Kumar, Khushu, Singh, & Gangenahalli, 2016). Comprehensively differentiating these two cell populations is difficult, but they do differ in their morphological and phenotypical classification.

Abbreviations: CCI, Cortical controlled impact; DAPI, 40,6-diamidino-2-phenylindole; dpi, days postinjury; GFAP, glial fibrillary astrocytic protein; hpi, hours postinjury; Iba-1, ionized calcium binding adaptor molecule 1; PBS, phosphate-buffered saline; TBI, traumatic brain injury; TUNEL, terminal deoxynucleotidyl transperase-mediated biotinylated UTP nick end labeling.

Typically, activated microglial cells appear hypertrophic/bushy with robust prolongations, while peripheral macrophages display an amoeboid morphology containing numerous vacuoles (Kettenmann et al., 2011). Depending on the grade of activation after brain injury, the MG/Mφ population can exhibit different functions and distinct metabolic stages. Studies have shown a "pro-inflammatory" MG/Mφ phenotype associated with the production of cytokines such as interleukin 1 beta (IL-1β), tumor necrosis factor alpha (TNFα), interferon gamma (IFNγ), and cluster of differentiation 40 (CD40) receptors; an "alternative activation" phenotype associated to the production of Arginase-1 (Arg1), interleukins 4 and 13 (IL-4, IL-13); and a "deactivated" phenotype associated with interleukin 10 (IL-10) or transforming growth factor beta 1 (TGFβ) which facilitate wound healing (Hsieh et al., 2013; Jin, Ishii, Bai, Itokazu, & Yamashita, 2012; Kumar, Alvarez-Croda, Stoica, Faden, & Loane, 2016a; Kumar et al., 2016b; Martinez & Gordon, 2014; Tang & Le, 2016). While a coordinated transition from a pro-inflammatory phenotype to an alternative or deactivated phenotype is hypothesized to facilitate the transition from acute brain injury response to neuron repair, emerging studies suggest that the switch between these stages has not been adequately established, and that cytokines classically defined as pro-inflammatory can also have anti-inflammatory properties, and vice versa (Durafourt et al., 2012; Martinez & Gordon, 2014; Orihuela, McPherson, & Harry, 2016; Selenica et al., 2013; Tang & Le, 2016). Indeed, following experimental TBI there is an overlapping expression of phenotypic markers in MG/Mφ (Kim, Nakamura, & Hsieh, 2016; Kumar et al., 2016a; Morganti, Riparip, & Rosi, 2016).

A recent review highlights the sparse and controversial background literature on sex-differences in mortality and functional outcome after TBI (Caplan, Cox, & Bedi, 2017), and it is clear that more studies are required to understand how sex affects neuroinflammatory mechanisms and outcomes after injury. However, the vast majority of the experimental preclinical TBI studies looking at the inflammatory response to TBI have been conducted using male animals. While it is known that females respond different to brain injury because of hormonal changes, the specific mechanisms underlying these sex differences remain elusive. Because of these challenges, the National Institutes of Health (NIH) are encouraging sexual diversity in preclinical research (McCullough et al., 2014). As far we are aware, this is the first study demonstrating the temporal and spatial differences in MG/Mφ activation following TBI, with a focus on morphological changes and cytokine mRNA production. Here, we report that the male/female MG/Mφ response shows complete divergence in the subacute phase postinjury with male mice displaying faster and more pronounced MG/Mφ activation and astrogliosis following moderate-to-severe TBI compared with female mice. In situ hybridization also reveals a divergent cytokine mRNA profile in MG/Mφ cells after injury. This is associated with early neuronal cell death and larger lesion volume in the first days postinjury in male compared with female mice. Our data suggest that pharmacological interventions that target the inflammatory cascade should consider sex differences as a significant variable following TBI.

2 | MATERIALS AND METHODS

2.1 | Animals and controlled cortical impact injury

We used young adult (9–14 weeks) male and female C57BL/6J mice (Jackson Laboratories, Bar Harbor, ME), housed under standard 12h light:dark cycle, five mice per cage, with open access to food and water. We used random cycling of female mice to better reflect clinical applicability. We housed five females per cage, isolated from male mice. To neutralize weight as a variable, we matched male and female mice for each group by weight. The average body weight at the time of the injury was 20.84 ± 0.33 g for males and 20.28 ± 0.20 g for females. Mice were also weighed at time of euthanasia, and there were no significant differences between males or females at all time-points (data not shown).

Mice were anesthetized with isoflurane (induction at 3% and maintained at 1.5%) evaporated in oxygen and administered through a nose mask. The mice were placed on a custom-made stereotaxic frame with a built-in heating bed that maintains body temperature at 37°C. A 10-mm midline incision was made over the skull to allow a 4 mm craniotomy on the left parietal bone. We performed moderate-to-severe controlled cortical impact (CCI) injury in the right somatosensory cortex target area (interaural 2 mm and bregma 2 mm) using a Leica Impact One Stereotaxic Impactor device (Leica Biosystems) to deliver the cortical impact, with a 3 mm diameter flat impact tip, impact velocity of 5.25 m/s, impact depth of 1.5 mm, and dwell time of 0.1 s. After injury, the incision was closed with staples and the mice were allowed to recover fully from anesthesia before transferring to their home cages. Sham injury consisted of exposure to anesthesia; stereotaxic mounting, skin and fascia reflection and incision closed using staples. All procedures were performed in accordance with protocols approved by the Georgetown University Animal Care and Use Committee. Mice were euthanized with CO_2 and transcardially perfused with phosphate buffer and decapitated at 4 h, 1, 3, 7, and 30 days postinjury (dpi). After postfixation of the brains in 4% paraformaldehyde overnight, brains were stored in a 30% sucrose solution for 48 h at 4°C. A sliding microtome (Microm HM 430, Thermo Fisher Scientific, Tusin, CA) was used to section the brains at 20 μm-thick in coronal orientation. The brain sections were then cryoprotected in an antifreeze solution (30% glycerol + 30% ethylene glycol + 40% 0.01 M phosphate-buffered saline (PBS)) for storage at – 20°C.

2.2 | Immunohistochemical techniques

Free-floating parallel sections were washed three times with PBS, before staining and incubated with blocking buffer (5% normal goat serum in PBS) and 0.3% Triton X-100 (PBST) for 2 h at room temperature. For the histological analysis of glial activation, brain sections were incubated overnight at 4°C with either one of the following primary antibodies: (a) polyclonal anti-rabbit Iba-1 antibody (1:500, Wako, Chemicals, Richmond, VA) for microglia/macrophages cells and (b) monoclonal anti-mouse GFAP antibody (1:1,000, Millipore, Temecula, CA) for astrocytes. After three 5 min washes in PBS, sections were

incubated with a corresponding anti-rabbit or anti-mouse Alexa Fluor 568-conjugated IgG secondary antibodies (1:1,000, Invitrogen, Carlsbad, CA) for 2 h at room temperature. For double labeling, sections were processed with polyclonal anti-rabbit P2Y12 (1:1,000, Anaspec, San Jose, CA) and polyclonal anti-rat F4/80 (1:200, R&D Systems, Minneapolis, MN) overnight at 4°C. As negative controls, sections were incubated in media lacking the primary antibody. After three 5 min washes in PBS, sections were incubated with a corresponding anti-rabbit Alexa Fluor 568-conjugated IgG and anti-rat Alexa Fluor 488-conjugated IgG secondary antibodies (1:1,000, Invitrogen) for 2 h at room temperature. Sections were rinsed with PBS three times and incubated in PBS with DAPI solution (1:50,000, Sigma-Aldrich, St. Louis, MO) for counterstained nuclei. The sections were rinsed with distilled water and coverslipped with Fluoro-Gel with Tris Buffer mounting medium (Electron Microscopy Sciences, Hatfield, PA).

2.3 | Densitometry and quantitative analysis of immunohistochemistry

For quantitative analysis of immunolabeled sections, we implemented unbiased standardized sampling techniques to measure tissue areas corresponding to the cortex, hippocampal dentate gyrus, and thalamus showing positive immunoreactivity (Villapol, Balarezo, Affram, Saavedra, & Symes, 2015; Villapol, Byrnes, & Symes, 2014) (Figure 1). To quantify the number of Iba-1 positive cells, an average of five single plane sections from the lesion epicenter (–1.34 to – 2.30 mm from bregma) were analyzed blind for each animal for each brain region (Figure 1a). Within each brain region, every Iba-1-positve cell in each of 5 (cortex), 2 (dentate gyrus), or 3 (dentate gyrus and thalamus) fields (x20, 151.894 mm^2) around the impact area ($n = 5$–6 mice/group at each time-point) (Figure 1b). Data are presented as the mean number of cells per mm^2. For proportional area measurements, the magnitude of the individual reaction for microglial and astroglial cells was reported as the proportional area of tissue occupied by immunohistochemical stained cellular profiles within a defined target area. Proportional area measurements do not necessarily reflect changes in actual cell numbers. Fluorescent images were acquired on an Axioplan 2 microscope (Zeiss, Thorwood, NY) with a Photometrics camera. Images were transferred to ImageJ64 software (NIH Bethesda, MD, USA), for inversion, thresholding, and densitometric analysis. The thresholding function is used to set a black and white threshold corresponding to the imaged field, with the averaged background subtracted out. Once a threshold is set, the "Analyze Particles" function can be used to sum up the total area of positive staining, and to calculate the fraction of the total area that is positive for the stain as previously was described (Villapol et al., 2014, 2015,). Data are shown as the percentage of Iba-1 or GFAP positive immunoreactivity per the total area that occupied on the field studied.

2.4 | Microglia and astrocyte morphologic assessment

Under physiological conditions, microglia exist in the "surveying" stage. In response to TBI, ramified microglia transform into activated nonpha-gocytic cells commonly referred to as "activated" microglia (Nimmerjahn, Kirchhoff, & Helmchen, 2005). To characterize the morphology of Iba-1 positive cells, we counted and classified the number of cortical microglial cells in each of the five MG/Mφ morphologic phenotypes (Ayoub & Salm, 2003; Doyle, Eidson, Sinkiewicz, & Murphy, 2017; Glenn, Ward, Stone, Booth, & Thomas, 1992; Kettenmann et al., 2011) in sham brains and injured brains at 4 h, 1, 3, 7, and 30 days after TBI. Morphological classification was based on a visual assessment of the MG/Mφ population. We used the following classifications (a) *ramified* (small cell body and long finely branched processes that extend in all directions from the perinuclear cytoplasm); (b) *ramified with rough prolongations* (first stage of microglia activation, phagocytic abilities); (c) *hypertrophy/bushy microglia with pseudopodia* (activated microglia demonstrate modest hypertrophy, and have limited, cytoplasmic extensions); (d) *amoeboid with phagocytosed cells* (macrophages or phagocytic microglia with fully retracted processes and clearly evident phagocytized debris); and (e) *amoeboid round* (macrophages or microglial-derived brain macrophages round in shape). An investigator that was blinded to the identity of the experimental groups performed morphometric analysis ($n = 5$–6 mice/group at each time-point).

2.5 | Fluorescent *in situ* hybridization combined with immunohistochemical labeling for microglia/ macrophages population

Coronal brain sections were mounted on gelatin-coated glass slides (Superfrost Plus, Thermo Fisher Scientific) and stored at – 80°C until use. Fluorescent *in situ* hybridization (FISH) was performed as per the manufacturer's instructions using RNAscope® Technology 2.0 Red Fluorescent kit for Fresh Frozen Tissue (Advanced Cell Diagnostics (ACD), Hayward, CA). All target probes consisted of 20 short double-Z oligonucleotide probe pairs that are gene specific and were obtained from ACD. For amplification and visualization, both Z-probes must bind to the mRNA of interest. Following probe hybridization, sections underwent a series of probe signal amplification steps followed by incubation of fluorescently labeled probes designed to target the Red channel associated (Figure 1h). Brain tissue sections were dehydrated by 50%, 70%, and 100% ethanol gradually for 5 min; boiled during 10 min with pretreatment 2 solution (citrate buffer), then they were incubated with pretreatment 3 solution (protease buffer) for 30 min before hybridization. Sections were then incubated at 40°C for 2 h with the following target probes for mouse: *Mus musculus interleukin 1 beta* (IL-1β) mRNA, (accession number NM_008361.3, target region 2-950); *Mus musculus Tumor necrosis factor alpha* (TNFα) mRNA, (accession number NM_013693.2, target region 41-1587); *Mus musculus transforming growth factor, beta 1* (TGFβ1) mRNA, (accession number NM_011577.1, target region 588-1913); *Mus musculus arginase* (Arg1) mRNA, (accession number NM_007482.3, target region 2-1114). A dapB probe targeting a bacterial gene was used as a negative control and Ppib (Mus musculus peptidylprolyl isomerase B mRNA; accession number NM_011149.2, target region 98-856) was used as a positive control. Positive hybridization consisted of a punctate signal representing a single mRNA target molecule, the color label was assigned to either FAR RED (Excitation
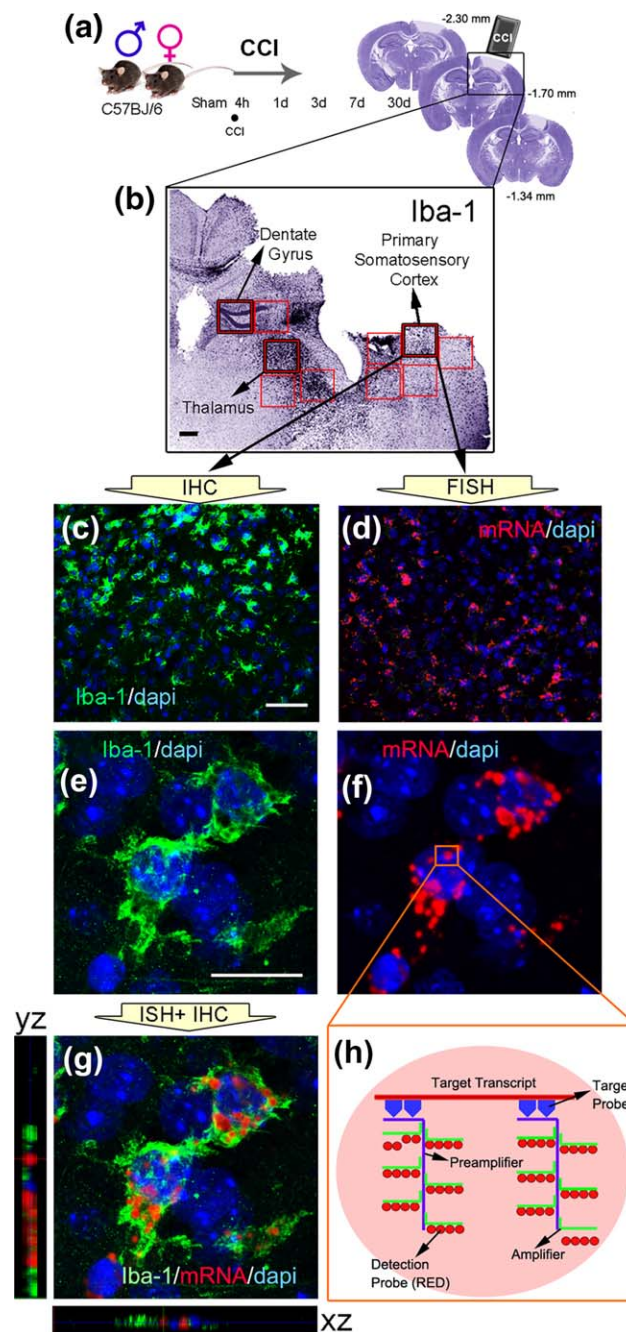
FIGURE 1 In situ hybridization combined with immunohistochemistry for analysis of the immune response in injured mouse brains. (**a**) Male and female C57BL/6J mice received a controlled cortical impact (CCI) injury and were sacrificed at 4 h, 1, 3, 7, or 30 days after CCI. Coronal mouse brains sections corresponding to the lesion area from −1.34 to −2.30 mm posterior to Bregma, Nissl stained, were selected for analysis. (**b**) Tissue was probed for microglia/macrophages cells (Iba-1, darker staining) and counterstained with nuclei (dapi, blue). Brain regions (primary somatosensory cortex, hippocampal dentate gyrus, and thalamus) used for quantification are outlined in this brain section micrograph (scale bar; 200 lm). (**c**) Representative image field of immunohistochemistry (IHC) of microglia/macrophages cells (Iba-1, green) and nuclei (dapi, blue), and (**d**) an example of mRNA expression (probe, red) corresponding to fluorescent in situ hybridization (FISH) using RNAscope (scale bar; 50 μm, for images c, d). (**e–g**) Microglia/Macrophage cells detected by IHC analysis with Iba-1 antibody (**e**, green) in the lesioned cortex exhibited strong FISH for a representative fluorescence probe (red) counterstained with nuclei (dapi, blue) (scale bar; 20 μm, for images e, f, g). RNAscope FISH produces puncta spike in signal (circle red) that represents a single mRNA transcript. The red square in **f** shows an image of a puncta signal, and the illustration depicted in **h** demonstrates the process of "Z" probes hybridizing with the target transcript, and subsequent fluorophore binding. [Color figure can be viewed at wileyonlinelibrary.com]

647 nm; Emission 690 ± 10 nm), (Figure 1, d, f, g). After FISH, slides were washed three times with PBS and blocking with PBST and 5% normal goat serum for 1 h. Immunofluorescence was performed using a mixture of primary antibodies to visualize the total MG/Mϕ population (Figure 1c, e, g); polyclonal anti-rabbit Iba-1 (1:500), polyclonal anti-rabbit P2Y12 (1:1,000) and polyclonal anti-rat F4/80 (1:200) overnight

at 4°C. Alexa Fluor 488-conjugated goat anti-rabbit, and anti-rat IgG (1:1,000, Invitrogen, Carlsbad, CA) were applied for 2 h at room temperature. Sections were rinsed with PBS three times and incubated in PBS with DAPI solution for counterstained nuclei. The sections were washed three times with distilled water and coverslipped with Fluoro-Gel with Tris Buffer mounting medium (Electron Microscopy Sciences).

2.6 | Quantification of immunofluorescence and FISH

Investigators blinded to the experimental conditions quantified FISH signal in three fields (x10, 514.560 mm^2) within the primary somatosensory cortex of four noncontiguous slices of the ipsilateral cortex (or cortical layer III-IV for sham mice) in a range of bregma -1.34 to -2.30 mm. The number of mRNA-positive cells that colocalized with DAPI nuclei were manually counted for IL-1β, TNFα, TGFβ, and Arg1. The negative probe used as a control did not contain any stained cells. The number of mRNA-positive/MG/Mϕ-positive cells, mRNA-positive/MG/Mϕ-negative cells, and the total number of MG/Mϕ cells were also quantified in four to six microscopic fields (x20, 151.894 mm^2) of view. A total of 15–20 counting frames were assessed per animal, and cells were evaluated for the presence of a labeled nucleus and expected cellular morphology as was previously described (Villapol, Wang, Adams, & Symes, 2013). In addition, the percentage of MG/Mϕ immunoreactive cells with different mRNA probes was also assessed ($n = 5$–6 mice/group at each time-point). The images were analyzed using AxionVision software and quantified using ImageJ64 software. Images were cropped and resized (if necessary) using Adobe Photoshop CS5, any changes to brightness and contrast settings were applied equally to the entire image, and to all corresponding images within the same dataset. A confocal microscope (Leica SP8) was used to take representative images from FISH-ISH brain sections using x20, x40, and x63 objectives.

2.7 | Cell death assay

Brain sections were processed for Terminal deoxynucleotidyl transferase-mediated biotinylated-dUTP nick-end labeling (TUNEL) staining was performed by using the *In situ* Cell Death Detection kit, Fluorescein (Roche, IL), according to the manufacturer's instructions. Coronal brain sections were mounted on gelatin-coated glass slides (Superfrost Plus). Briefly, cryosections were rinsed with PBS and were incubated with kit-supplied TUNEL reaction mixture at 37°C for 1 h. For double-staining, cryosections were incubated with primary antibody against monoclonal anti-mouse Neurofilament 200 (NF200) (1:200, Sigma-Aldrich) overnight at 4°C, Alexa Fluor 568-conjugated goat anti-mouse IgG (1:1,000, Invitrogen) were applied for 1 h at room temperature. Sections were rinsed with PBS three times and incubated in PBS with DAPI solution for counterstained nuclei. The sections were washed three times with distilled water and coverslipped with Fluoro-Gel with Tris Buffer mounting medium (Electron Microscopy Sciences). TUNEL-positive nuclei were counted in cortical regions (x20) in the three to five coronal sections for each animal ($n = 5$–6 mice/group at each time-point).

2.8 | Histological nissl stain and lesion volume measurements

Nissl staining was assessed on an average of 13 brain sections spaced equidistant apart, between 0 and -2.70 mm from bregma corresponding to the injured area. Brain slices were mounted on gelatin-coated glass slides (Superfrost Plus) and stained for 5 min with 1% Cresylviolet (Sigma-Aldrich) dissolved in distilled water and filtered. Slides stained were dehydrated for 2 min using 100%, 95%, 70%, and 50% ethanol, cleared in xylene for 2 min, covered with Permount mounting medium (Thermo Fisher Scientific) and coverslipped. The lesion volume was calculated by multiplying the sum of the lesion areas by the distance between sections. Lesion percentage was calculated by dividing each lesion volume by the total contralateral hemisphere volume (Villapol et al., 2012).

2.9 | Statistical analyses

Data were analyzed using two-way analysis of variance (ANOVA) with Bonferroni post hoc test using GraphPad Prism software v. 5.0 (Graphpad). A p-value < 0.05 was considered statistically significant. Quantitative data for all figures and tables are expressed as mean $\pm$ SEM.

3 | RESULTS

3.1 | Sex dimorphism in MG/Mϕ activation after TBI

Previous reports have consistently demonstrated a role for microglial activation in the pathophysiology of TBI, however, the impact of sex differences on this response is unknown. Using immunohistochemistry, we detected Iba-1 positive cells and determined their number, area occupied and morphology in several injured brain regions of adult male and female mice at several time-points after TBI. We report that the total Iba-1-positive area was significantly higher in male mice in the primary somatosensory cortex (306.2% and 172.90% increase in male vs. female mice at 1 and 3 dpi, respectively; Figure 2a–c), in the dentate gyrus (240.4%, 225.3%, and 129.8% increase in male vs. female mice at 1, 3, and 7 dpi, respectively; Figure 2d–f), and in the thalamus (158.4% and 149.4% increase in male vs. female mice at 1 and 3 dpi, respectively; Figure 2g–i). For quantitative analysis, we focused on the primary somatosensory cortex region, located immediately adjacent to the injury site (Figure 1b). We found that TBI in male mice caused a rapid increase in the number of Iba-1 cells beginning at 1 dpi, but female mice did not increase Iba-1 cells until 7 dpi—suggesting decreased MG/Mϕ infiltration/proliferation at the acute phase posttrauma (Figure 2j). Male and female mice had a similar number of MG/Mϕ cells at 30 dpi in all brain regions. Next, we determined the morphological status of the MG/Mϕ into (a) ramified, (b) ramified with thick, rough prolongations, (c) hypertrophic/bushy with pseudopodia, (d) amoeboid with phagocytosed cells, or (e) amoeboid round cells (Figure 2k–o). Following sham-injury, 100% of the MG/Mϕ were classified as ramified, displaying small cell bodies with thin, long, and highly branched processes. In both sexes, TBI caused a time-dependent
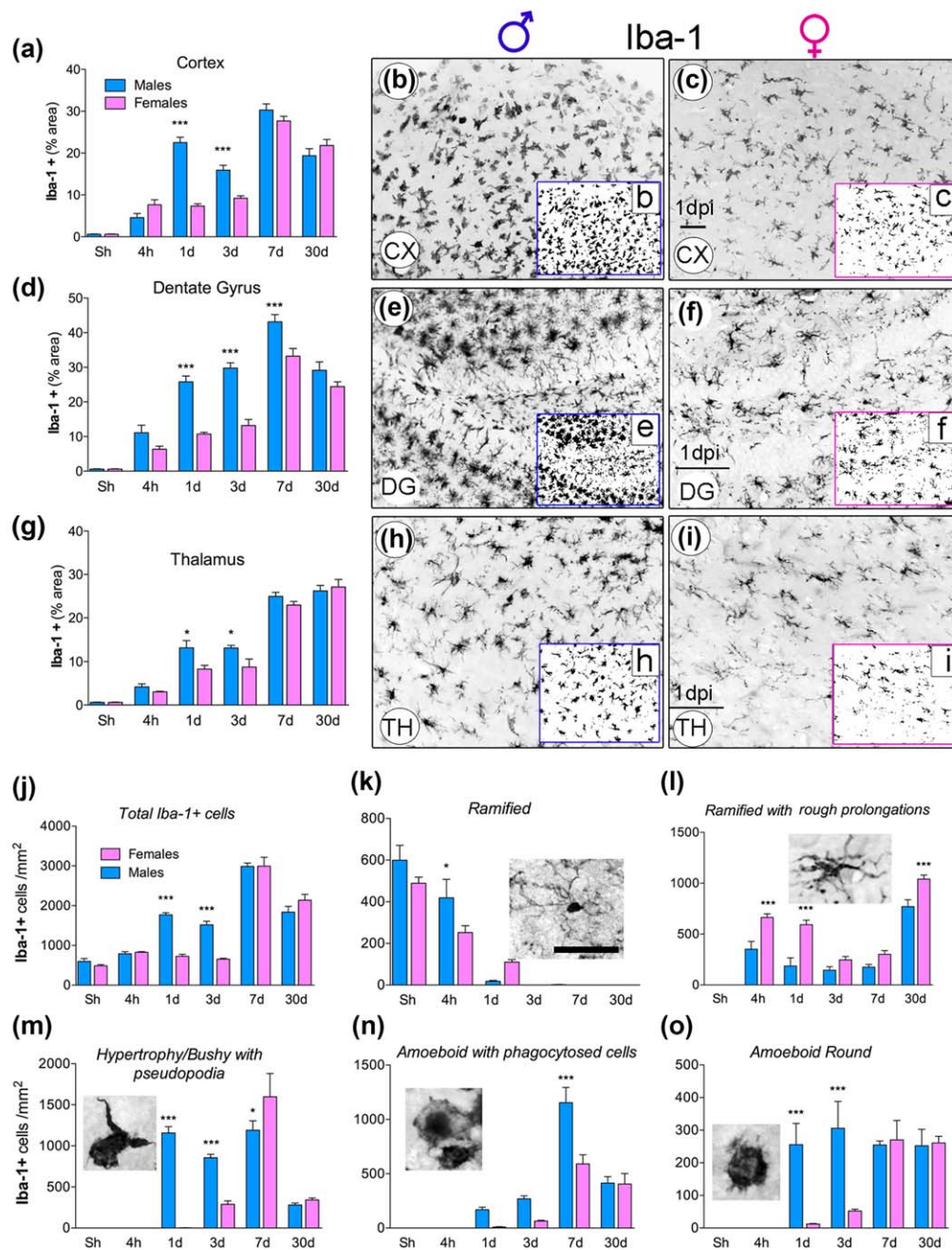
FIGURE 2 Sex-dependent differences in microglia/macrophage morphology and activation after TBI. **a-c** TBI causes an increase in Iba-1 positive cell area in the cortex (CX) of male mice that is stronger than the response in female mice. Representative images of Iba-1 immunohistochemical staining show an increase in microglial/macrophages cells in male mice compared with female mice at 1-day postinjury (dpi) (CX). Sex-differences are also observed in the hippocampal dentate gyrus (DG; **d-f**), and thalamus (TH; **g-i**), (Scale bar; 50 μm). Inset images **(b, c, e, f, h, i)** are corresponding thresholded images used to quantify the percentage area occupied by Iba-1 positive cells. **(j-o)** A number of Iba-1 positive cells is classified according to microglial morphology in the primary somatosensory cortex located in the perilesional brain regions. Representative photos in each graph are depicting the five classifications of microglia/macrophage morphology (ramified; ramified with thick, rough prolongations; hypertrophy/bushy with pseudopodia; amoeboid with phagocytized cells; and amoeboid round). The total number of Iba-1 positive cells per mm^2 **(j)** is higher in males compared with females at 1 and 3 dpi. We observed ramified morphology (**k**, inset representative image) in sham brains with long processes at 4 h postinjury (hpi), absent at later times; the ramified morphology with rough prolongations (**l**, inset representative image) is higher in females at 4 hpi and 1 dpi compared with male injured brains, decreasing at 3 and 7 dpi, reaching a peak at 30 dpi but without sex differences. We found hypertrophy/bushy Iba-1 positive cells with pseudopodia (**m**, inset representative image) at 1 and 3 dpi in male brains but rarely in females until 7 dpi, microglia retract most of their processes and show enlargement of cell bodies. Amoeboid cells with phagocytosed cells **(n**, inset representative image) were found mainly in male brains, reaching a peak at 7 dpi, compared with female brains. Amoeboid round morphology (**o**, inset representative image) was typically present in males at 1 and 3 dpi and absent in females, with sex equivalence at 7 and 30 dpi. In chronic stages, the majority of the microglia/macrophages still had increased cell body size and fewer processes when compared with sham mice. Scale bar for inset representative images 20 μm. * = $p < 0.05$; *** = $p < 0.001$ vs. females at the same time-point. $n = 5$/group. [Color figure can be viewed at wileyonlinelibrary.com]
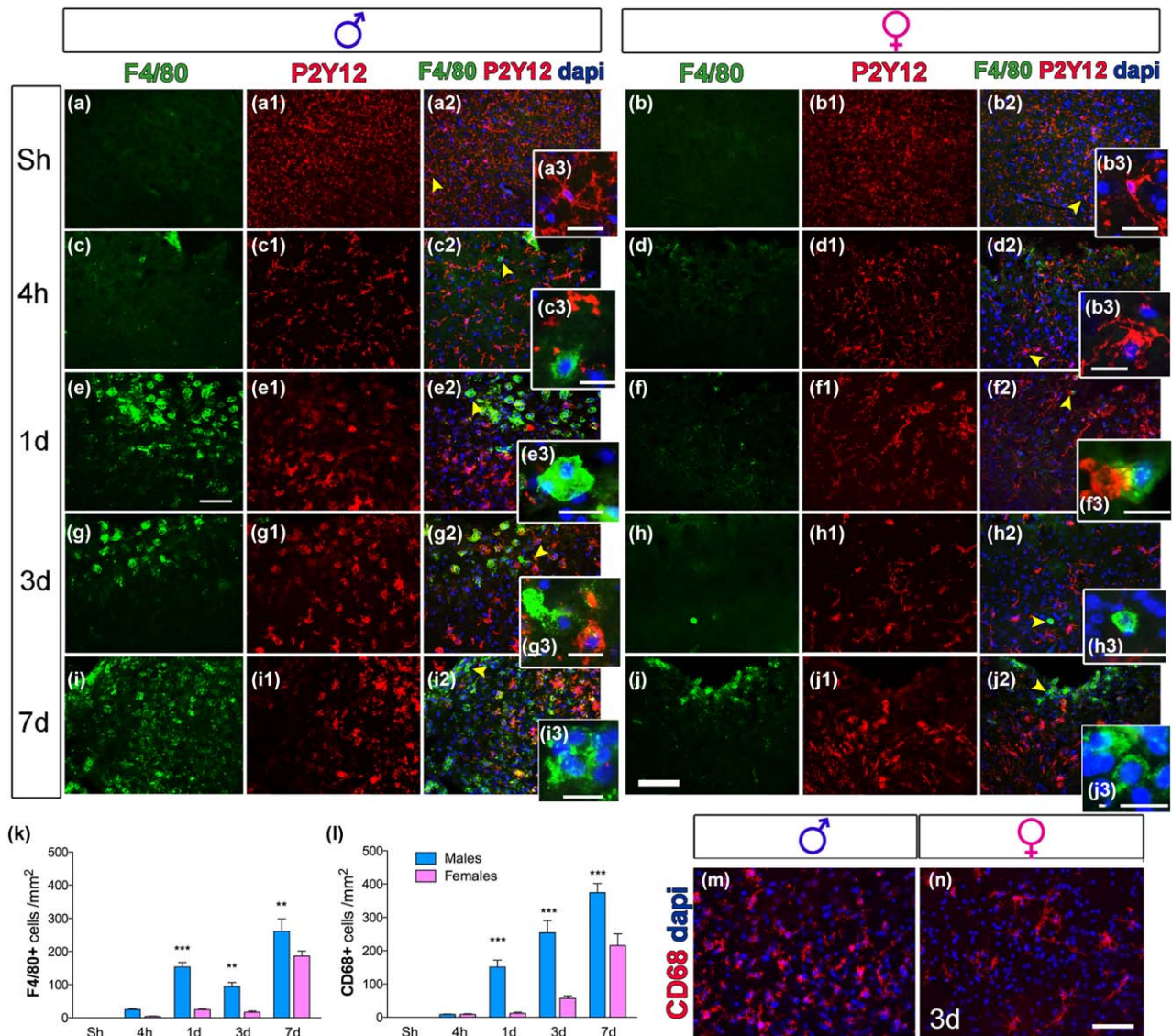
FIGURE 3 Male, but not female, TBI mice have rapid infiltration of macrophages into the injured brain. Representative images indicate cortical brain sections stained with P2Y12 (resident microglial cells, red) and F4/80 (macrophages, green) markers, and nuclei counterstained with dapi (blue). No F4/80 positive cells were observed in sham (Sh) male mice (**a, a1–a3**), sham female mice (**b, b1–b3**), 4h TBI male mice (**c, c1–c3**), or 4h TBI female mice (**d, d1–d3**). F4/80 positive macrophages with amoeboid morphology predominantly appear at 1 dpi in the perilesional cortex of male mice (**e, e1–e3**) but remain absent in female brains (**f, f1–f3**). F4/80 positive macrophages persist at 3 dpi in male brains (**g, g1–g3**) and appear a few in female brains (**h, h1–h3**). By 7 dpi F4/80 positive macrophages are widespread in the injured cortex of male mice (**i, i1–i3**), and are apparent around the lesion in female TBI brain (**j, j1–j3**). Quantitative graphs indicate an increase in F4/80 positive macrophages (**k**) and CD68 positive activated microglia/macrophages cells (**l**) in males compared with females at all time-points. Representative images of CD68 positive cells (red) staining and nuclei (dapi, blue) are showing for males (**m**) and females (**n**) at 3 dpi. Scale bars for images 50 μm, and for high-power magnification boxes 20 μm. ** = $p < 0.01$; *** = $p < 0.001$ vs. females at the same time-point $n = 5$/group. [Color figure can be viewed at wileyonlinelibrary.com]

change in MG/Mφ morphology with the number of ramified microglia in the primary somatosensory cortex being completely abolished by 3 dpi (Figure 2k). Female mice had higher numbers of ramified MG/Mφ with thick rough prolongations at 4 h and 1 dpi (Figure 2l). At 1 and 3 dpi, male mice had significantly higher numbers of hypertrophy/bushy MG/Mφ with pseudopodia (Figure 2m), and significantly higher amoeboid MG/Mφ with phagocytosed cells at 7 dpi (Figure 2n), and significantly higher amoeboid round MG/Mφ (Figure 2o).

3.2 | Rapid activation and infiltration of MG/Mφ to the injured cortex occurs in male, but not female mice

TBI induces the rapid infiltration of blood-derived peripheral immune cells into the brain. We used a combination of membrane-specific markers and morphological changes to determine if the Iba-1-labeled cells with large phagocytic vacuoles/vesicles could be infiltrating cells. F4/80 is a well-characterized membrane protein highly expressed on macrophages, and F4/80-positive macrophages have been shown to
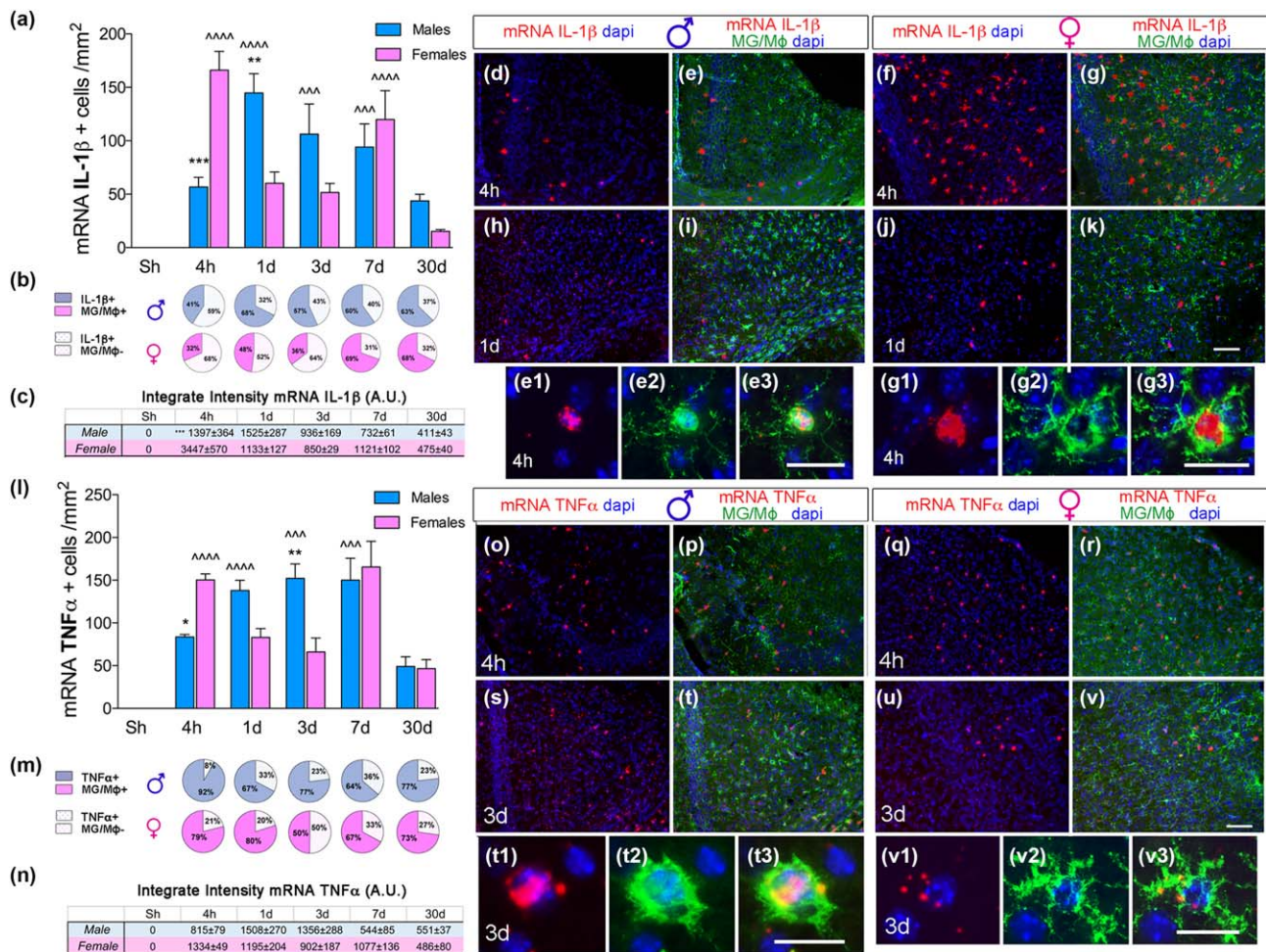
FIGURE 4 Sex-specific IL-1β and TNFα cytokine expression after TBI. (**a**) Increased IL-1β positive cells in the injured cortex in female mice compared with males at 4-h postinjury, but increased expression in males at 1 and 3 days postinjury. (**b**) Total IL-1β positive cells expressed in microglia/macrophage cells (MG/Mϕ) vs. non-MG/Mϕ in the cortex of male and female brain at each time point after TBI. (**c**) Average mRNA IL-1β expression determined by fluorescent intensity in the cortex of males and females after TBI. (**d–k**) Representative images for IL-1β positive cells (red), MG/Mϕ (green) and nuclei (dapi, blue) in the cortex of male (**d, e, e1–e3**) and female mice (**f, g, g1–g3**) at 4h, and male (**h, i**) and female mice (**j, k**) at 1d postinjury. Scale bar 50 μm for D–K; and 20 μm for e1-e3 and g1-g3. (**l**) Female mice have more TNFα positive cells at increased levels in the injured cortex at 4 h compared with male mice, but male mice have more TNFα positive cells at 1 and 3d compared with females. (**m**) TNFα positive cells expressed in MG/Mϕ vs. non-MG/Mϕ in the cortex of male and female brain after TBI. (**n**). Average mRNA TNFα expression determined by fluorescent intensity in the cortex of males and females after TBI. (**o–v**). Representative images for TNFα positive cells (red), MG/Mϕ (green) and nuclei (dapi, blue) in the cortex of male (**o, p**) and female mice (**q, r**) at 4 hpi, and male (**s, t, t1–t3**) and females (**u, v, v1–v3**) at 3 dpi. Scale bar 50 μm for D–K; and 20 μm for e1–e3 and g1–g3. * = $p < 0.05$; ** = $p < 0.01$; *** = $p < 0.001$ vs. female mice at the same time-point. ^^^= $p < 0.001$; ^^^^= $p < 0.0001$ vs. sham mice of the same sex. $n = 5/6$ group. [Color figure can be viewed at wileyonlinelibrary.com]

rapidly infiltrate the injured cortex following TBI (Hsieh et al., 2013; Kumar et al., 2016a; Morganti et al., 2015). To discern the total MG/Mϕ population, we also used the P2Y12 maker, a known membrane marker that distinguishes microglia from other myeloid lineage cells; its expression is limited to the ramified processes of microglia (Moore et al., 2015), however, P2Y12 was also identified in activated microglia (Ohsawa et al., 2010; Ohsawa & Kohsaka, 2011). Sham-injured male and female brains both had P2Y12-positive microglia, with no evidence of F4/80-positive cells in the somatosensory cortex (Figure 3a–a2, b–b2, k). Within 4 h postinjury, F4/80 positive macrophages remained rare (Figure 3c,d) in the injured

cortex. Male mice displayed a significant increase in F4/80-positive cells at 1 and 3 dpi that did not occur in female mice (Figure 3e–h, k). Infiltrating macrophages were evident in female mice at 7 dpi and were not significantly different to F4/80 cell number in male mice at this time-point (Figure 3i–k). By 30 dpi there were no F4/80 cells in either male or female mice (data not shown). We also performed immunofluorescence to detect CD68, a marker of highly activated and phagocytic myeloid cells that include both microglia and macrophages (Figure 3l–n). We again found that male mice had significantly higher numbers of CD68-positive cells at 1, 3, and 7 dpi (Figure 3l) compared with females (Figure 3l–n).
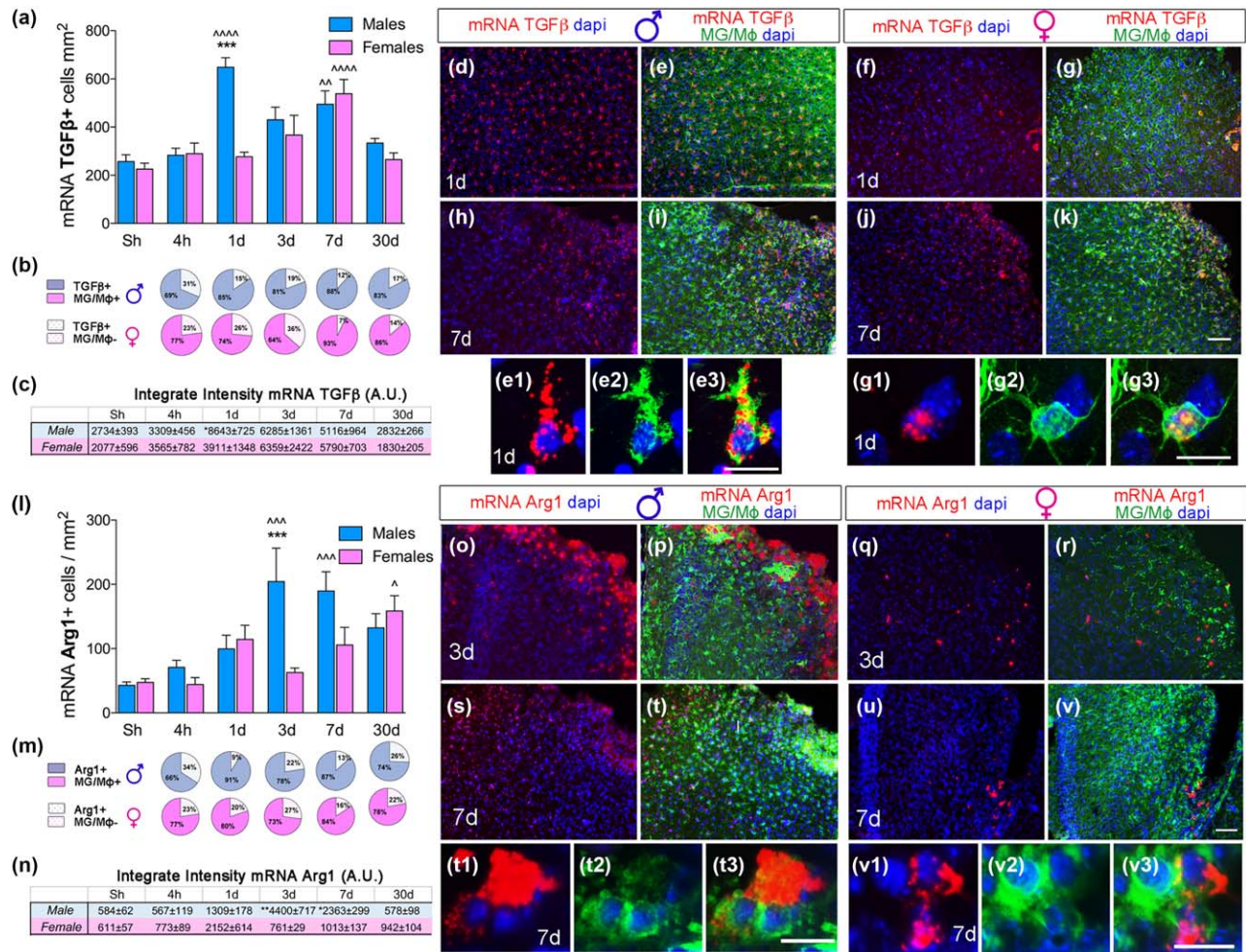
FIGURE 5 TGFβ and Arg1 cytokines expression by activated microglia/macrophages predominate in males after brain injury. (**a**) TGFβ positive cells in the injured cortex significantly increased in males compared with females at 1-day postinjury (dpi). (**b**) Percentage of total TGFβ positive cells expressed in microglia/macrophage cells (MG/Mφ) vs. non-MG/Mφ in the cortex of males and females at each time point after TBI. (**c**) Table shows the integrate intensity of TGFβ mRNA expression in the cortex of males and females after TBI. (**d–k**) Representative images for TGFβ positive cells (red), MG/Mφ (green) and nuclei (dapi, blue) in the cortex of males (**d, e, e1–e3**) and females (**f, g, g1–g3**) at 1 dpi, and males (**h, i**) and females (**j, k**) at 7 dpi. Scale bar 50 μm for D-K; and 20 μm for e1–e3 and g1–g3. (**l**) Arg1 positive cells in the injured cortex are significantly increased in males at 3 and 7 dpi compared with females. (**m**) Percentage of total Arg1 positive cells expressed in MG/Mφ vs. non-MG/Mφ in the cortex of males and females brains per each time point after TBI. (**n**) The table shows the integrate intensity of Arg1 mRNA expression in the cortex of males and females after TBI. (**o–v**) Representative images for Arg1 positive cells (red), MG/Mφ (green) and nuclei (dapi, blue) in the cortex or males (**o, p**) and females (**q, r**) at 3 dpi, and males (**s, t, t1–t3**) and females (**u, v, v1, v2, v3**) at 7 dpi. Scale bar 50 μm for d–k and o–v; and 20 μm for e1–e3, g1–g3, t1–t3, and v1–v3. * = $p < 0.05$; ** = $p < 0.01$; *** = $p < 0.001$ vs. female mice at the same time-point. ^^^ = $p < 0.001$; ^^^^ = $p < 0.0001$ vs. sham mice of the same sex. $n = 5$–6/group. [Color figure can be viewed at wileyonlinelibrary.com]

3.3 | Sex differences in pro-inflammatory cytokine expression after TBI

RNAscope FISH in combination with immunofluorescence was performed on brain sections collected from male and female mice. Females had significantly higher levels of IL-1β cytokines at 4 h post-TBI, compared with males (Figure 4a), suggesting that the IL-1β expression in response to injury within the male and female brain may be functionally, or biochemically, distinct. There was no detectable IL-1β expression in sham animals, while approximately 50% of cells expressing IL-1β were detected in MG/Mφ (see plots in Figure 4b). Collectively, these data show that IL-1β mRNA expression within the male and

female brains is not only produced by the MG/Mφ population, but also by other glial cell types or neurons (Choi & Friedman, 2009; Srinivasan, Yen, Joseph, & Friedman, 2004). Additionally, mRNA IL-1β expression intensity was sex-specific in IL-1β positive cells, within high levels in MG/Mφ of females at 4 h compared with males, and an inverse mRNA IL-1β MG/Mφ expression profile at 1 and 3 dpi (Figure 4c). In accordance with this data, females had increased mRNA TNFα expression compared with males at 4 h post-TBI, whereas males had significantly increased mRNA TNFα expression at 3 dpi compared with females (Figure 4l). There was no detectable TNFα expression in sham-operated animals. Approximately 70% of TNFα positive cells colocalized with MG/Mφ (see plots in Figure 4m). Additionally, we determined the
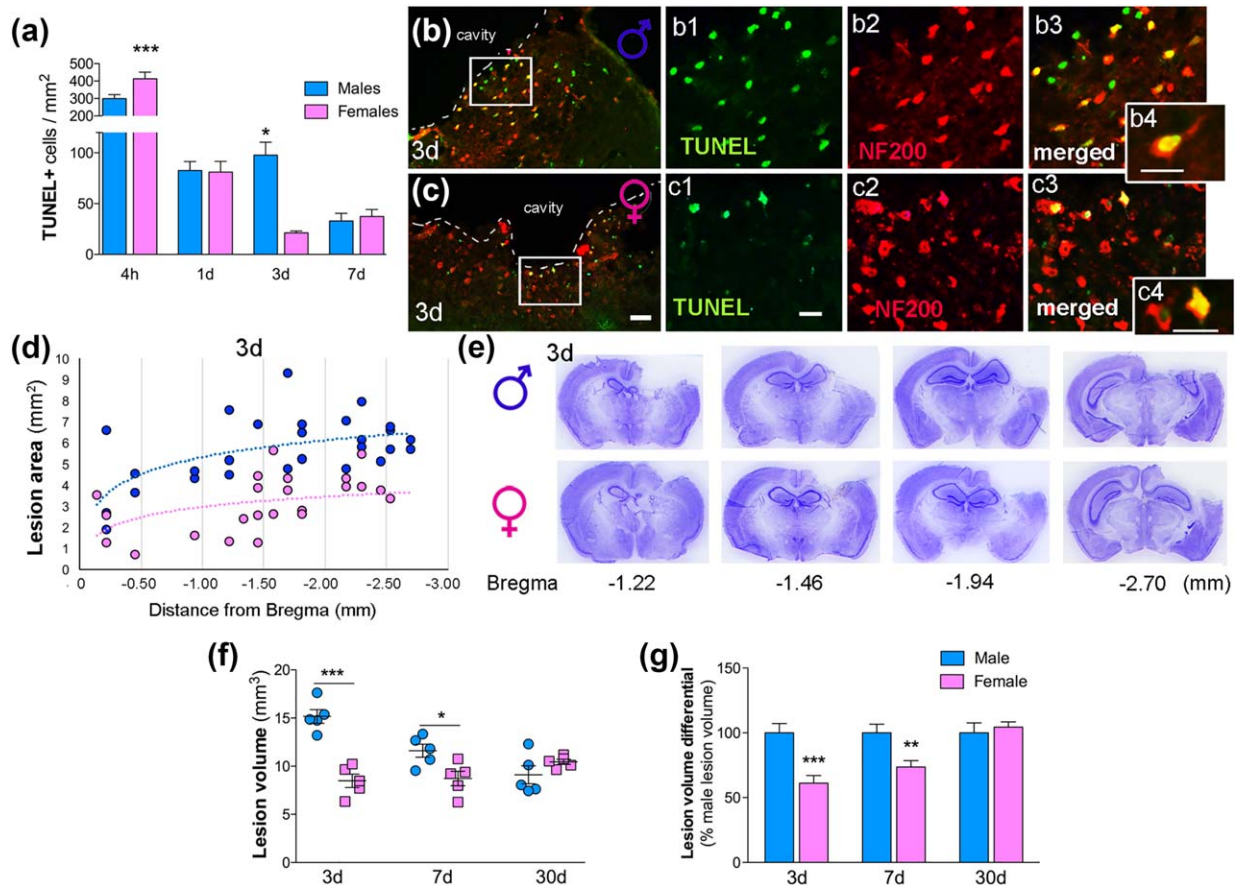
FIGURE 6 Female mice have reduced cell death and lesion volume acutely after TBI compared with male mice. (**a**) A peak in cell death was observed at 4 h postinjury (hpi), which resolved in female mice quicker than male mice. At 3 days postinjury (dpi), male mice had significantly higher numbers of TUNEL-positive cells compared with females. Representative images for TUNEL (green), NF200 (neurons, red) and a merged image in male (**b, b1–b4**) and female (**c, c1–c4**) injured cortex, respectively. Scale bars for b and c; 50 μm, for b1–b3 and c1–c3; 20 μm, and high magnification insets (b4, c4) 20 μm. (**d, e**) Detailed analysis of lesion volume in 3 dpi mice and representative Cresyl-violet images with their distance from Bregma. (**f**) Lesion volume in male and female mice at 3, 7, and 30 dpi. (**g**) Female lesion volume represented as percentage of male lesion volume at the same time-point. * = $p < 0.05$; ** = $p < 0.01$; *** = $p < 0.001$ vs. female mice at the same time-point. $n = 5$/group. [Color figure can be viewed at wileyonlinelibrary.com]

collective intensity levels of mRNA TNFα expression showed no sex discrepancies. MG/Mφ localization and TNFα positive cell distribution in the ipsilateral cortex cells in males and females is shown in Figure 4o, p, s, t, t1–t3 and Figure 4 q, r, u, v, v1–v3, respectively. By 7 dpi, male and female TBI mice had similar expression profiles of both pro-inflammatory IL-1β and TNFα mRNAs (Figure 4a, l).

3.4 | Anti-inflammatory cytokines are predominantly expressed in males after brain injury

The expression profiles of TGFβ, a marker of immunoregulatory cells, and Arg1, a marker of alternatively activated cells, were analyzed in the cortex of males and female mice. Following TBI we observed an increase in the production of TGFβ in males, but not in females, at 1 dpi compared with sham mice. Peak expression of TGFβ was observed at 7 dpi, but no sex-dependent differences were observed (Figure 5a). Approximately 80% of TGFβ positive cells colocalized with MG/Mφ (Figure 5b). These results demonstrated that a high percentage of MG/Mφ cells express TGFβ and that the remainder of cells correspond to

astrocytes and/or vessels (data not shown). Furthermore, TGFβ expression levels demonstrate a strong correlation in the pattern of TGFβ expression per mm² in both male and female animals (Figure 5c). An increase in the Arg1 levels was found only in the ipsilateral cortex of male mice at 3 dpi, continuing up to 7 dpi. Female mice did not show similarly robust increased expression levels (Figure 5l). In addition, the observed sex difference was not found in sham-injured mice. Approximately 70–90% of Arg1 positive cells were detected in MG/Mφ, across all time-points (Figure 5m). With respect to Arg1 expression, mRNA Arg1 was predominantly produced by MG/Mφ cells that displayed an amoeboid morphology (Figure 5 t1–t3). Furthermore, mRNA Arg1 expression levels were significantly higher in male compared with female mice at 3 and 7 dpi (Figure 5n), respectively.

3.5 | Cell death is time and sex dependent following TBI

We examined TBI-induced neuronal cell death in the pericontusional cortex, adjacent to the impact. At 4 h after injury, we observed 38%
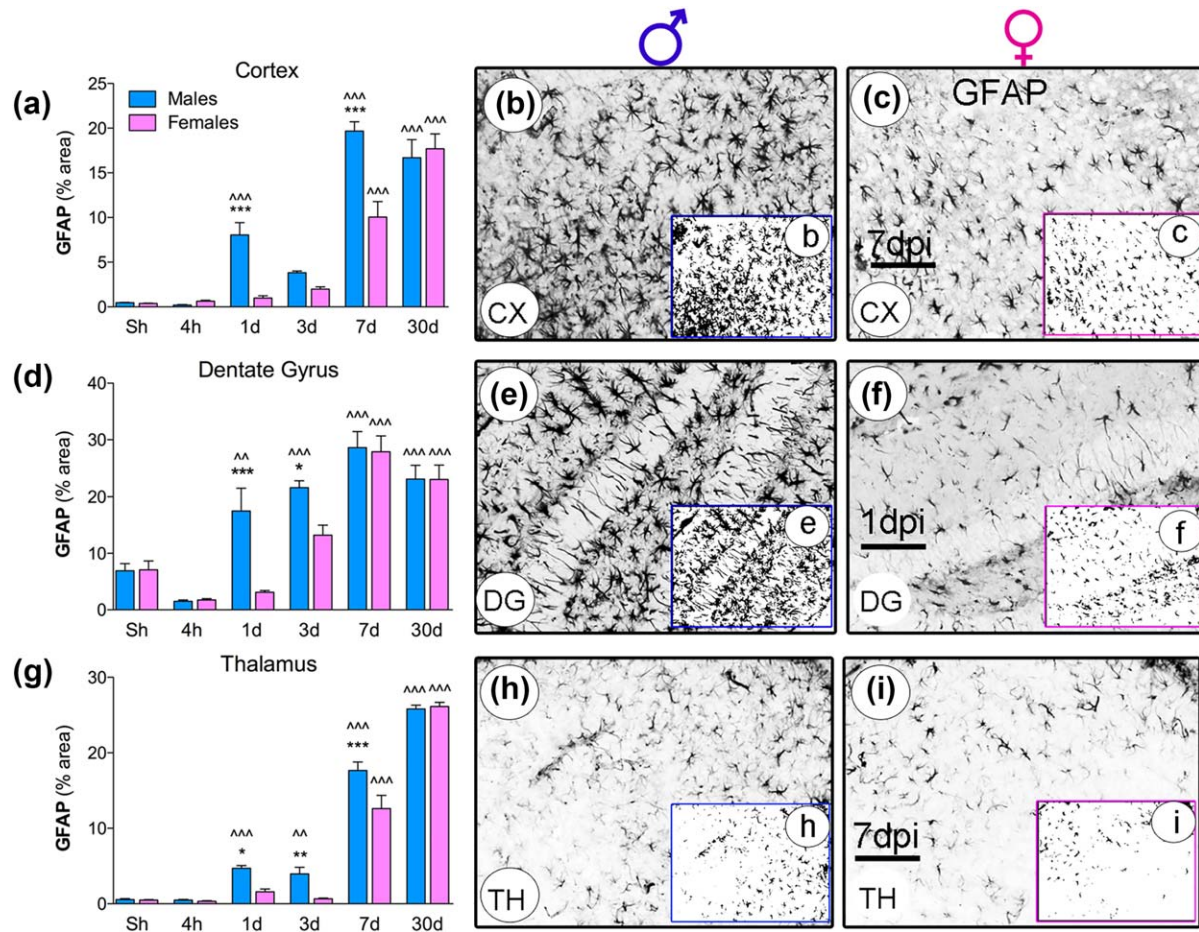
FIGURE 7 TBI induces a rapid astroglial response in male, but not female, mouse brain. Immunohistochemical staining of GFAP reveals rapid astrocyte activation in male mouse brain mice compared with females in the primary somatosensory cortex (CX; **a–c**); hippocampal dentate gyrus (DG; **d–f**), and thalamus area (TH; **g–i**), (Scale bar; 50 μm). Inset images (**b, c, e, f, h, i**) correspond to a thresholded image field to measure the percentage of area occupied by GFAP positive astrocytes. Scale bar; 50 μm. * = $p < 0.05$; ** = $p < 0.01$; *** = $p < 0.001$ vs. female mice at the same time-point. ^^^= $p < 0.001$; ^^^^= $p < 0.0001$ vs. sham mice of the same sex. $n = 5$/group. [Color figure can be viewed at wileyonlinelibrary.com]

more TUNEL positive cells in female compared with male mice (Figure 6a). There were no sex-dependent differences in TUNEL cell number at 1 dpi, however, at 3 dpi, there was a 358% increase in TUNEL positive neurons in males compared with females in the pericontusional cortical regions (Figure 6a–c). This translated into significantly larger infarct area in male mice compared with female mice at 3 dpi (Figure 6d, e). Overall, lesion was 64% larger in male mice at 3 dpi and 36% larger at 7 dpi compared with female mice (Figure 6f, g). Lesion volume at 30 dpi was similar between male and female mice (Figure 6f, g).

3.6 | Acute astrogliosis occurs in male, but not female, mice after TBI

We used GFAP immunohistochemistry to assess the temporal and spatial distribution of astrogliosis in males and female brains following TBI. We found that the immunoreactive area occupied by GFAP positive astrocytes was higher in males compared with females at 1 and 7 dpi in the ipsilateral cortex (833% and 196%, respectively) (Figure 7a–c), at 1 and 3 dpi in the ipsilateral hippocampal dentate gyrus (560% and

163%, respectively) (Figure 7d–f), and in the ipsilateral thalamus at 1, 3, and 7 dpi (297%, 629%, and 140%, respectively) (Figure 7g–i). For all areas studied, astrogliosis was not significantly different between male and female mice at 30 dpi.

4 | DISCUSSION

There are limited studies on the effect of sex on inflammation after CNS injury, and in this study, we examine the spatial and time-dependent neuroinflammatory changes that occur after experimental TBI. We report that after brain injury, male mice have a faster and more robust MG/Mφ activation and peripheral macrophage recruitment compared with females (Figure 8). This leads to increased cell death and lesion volume in the first week postinjury. However, beyond the first week postinjury, the female inflammatory response accelerates to become indistinguishable from that of males. While we can detect sex-differences in lesion volume acutely after injury, we observe identical brain tissue loss at 1-month postinjury. Previous clinical and animal
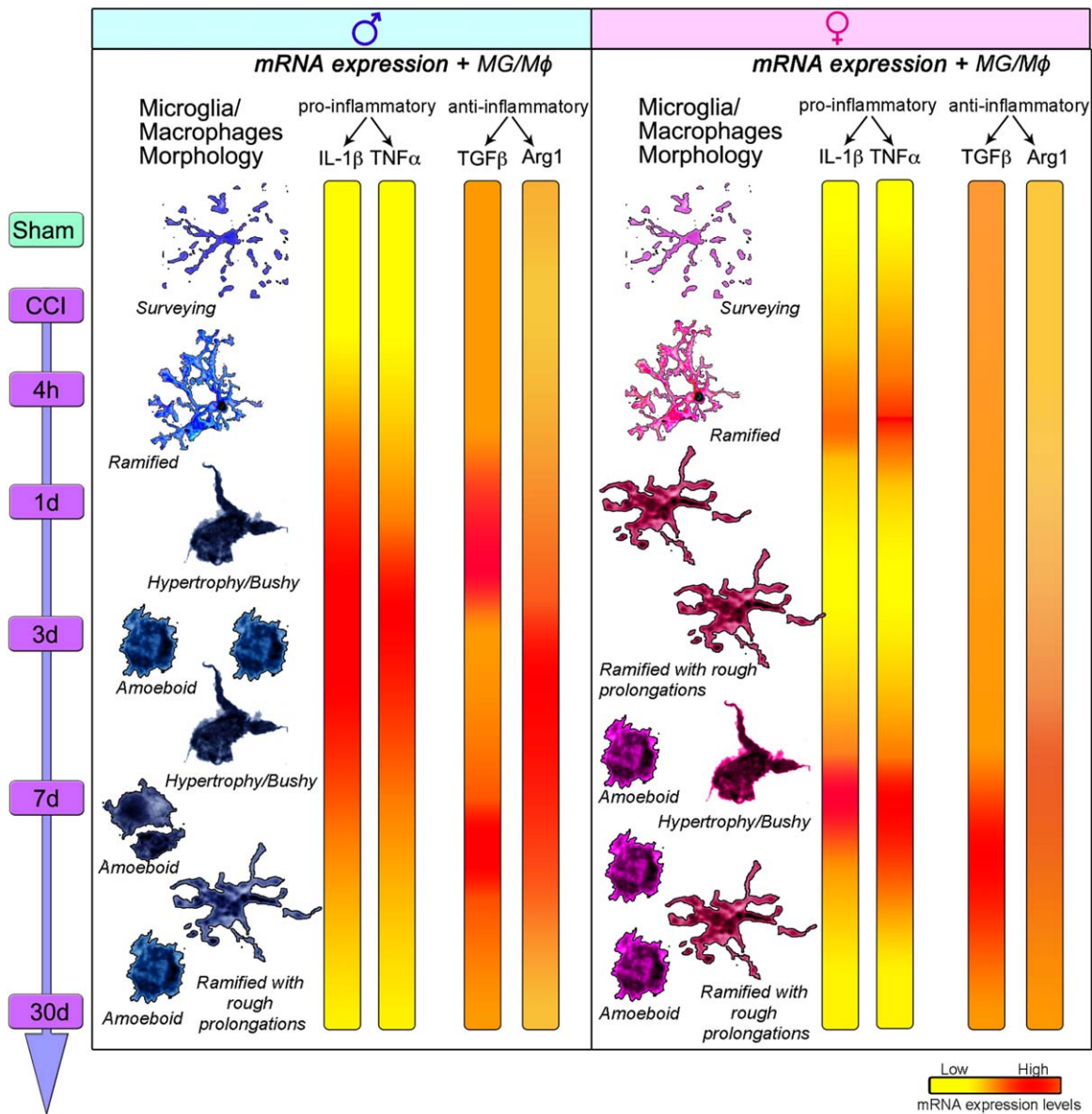
FIGURE 8 Sex differences in morphological and phenotypic diversity of microglia/macrophages following TBI. Schematic diagram illustrating the characterization of M1/M2-like microglia/macrophage cells (MG/Mφ) in males and females. Both sham male and female brains present surveying microglia and basal levels of cytokines. Days after injury, male mice have increased levels of infiltrating macrophages and activated microglial cells with hypertrophied/bushy morphology. One week after injury, MG/Mφ predominate in both sexes. In the frame time where macrophage infiltration occurs, the peak of cytokine expression is increased in males, while reduced in females. Both phenotypes, pro-inflammatory (IL-1β and TNFα) or anti-inflammatory (TGFβ and Arg1) activation status, in response to injury are more prevalent in injured male brains compared with females. [Color figure can be viewed at wileyonlinelibrary.com]

studies have demonstrated that sex-differences in mortality and functional outcomes exist after TBI (Caplan et al., 2017), and the use of hormone-based therapies in preclinical studies clearly show that female sex hormones, estrogen, and progesterone, are protective after TBI (Engler-Chiurazzi, Brown, Povroznik, & Simpkins, 2016; Stein, 2015). One of the major targets of estrogen and progesterone is the inflammatory response, and *in vitro* and *in vivo* studies demonstrate that these hormones can attenuate microglial activation and pro-inflammatory cytokine release (Arevalo, Santos-Galindo, Acaz-Fonseca, Azcoitia, & Garcia-Segura, 2013; Belcredito et al., 2001; Bruce-Keller et al., 2000, 2007; Crain, Nikodemova, Watters, 2013;

Dimayuga et al., 2005; Goodman, Bruce, Cheng, & Mattson, 1996; Habib & Beyer, 2015; Sawada et al., 2000; Vegeto et al., 2001). Here we studied how sex altered the inflammatory response following moderate-to-severe TBI with a focus on MG/Mφ number, morphology, and cytokine mRNA profile.

Microglia are dynamic immune cells whose number and morphological changes are closely associated with their functional activity (Ohsawa & Kohsaka, 2011; Stence, Waite, & Dailey, 2001; Tam & Ma, 2014). We found that TBI caused a rapid increase in the total number of Iba-1 immunopositive cells in male mice that was significantly faster than the response in female mice. These cells were also much larger on

average, with male Iba-1 immunopositive cells having a larger area than female cells through 7 dpi. These data are in agreement with previous results studying stab injury, where an injury induced a greater density of Iba-1 cells in the lesion border in male mice at 7d post-TBI compared with female mice (Acaz-Fonseca, Duran, Carrero, Garcia-Segura, & Arevalo,. 2015).

Morphologically, microglia in the un-injured brain have numerous, thin, ramified processes that survey the local tissue microenvironment, and following acute CNS insult microglia rapidly transform into an activated phenotype with distinct hypertrophic or bushy morphologies (Faden, Wu, Stoica, & Loane, 2016; Jin et al., 2012; Schnell, Fearn, Klassen, Schwab, & Perry, 1999). We observed sexual dimorphism in the morphological changes that occurred after TBI, with hypertrophic/amoeboid/phagocytic MG/Mϕ being more predominant in males compared with females. Morphological changes in MG/Mϕ phenotypes could be a determinant factor in activation of the inflammatory cascade, involving the expression of a broad range of surface receptors that allows them to sense subtle changes in the microenvironment and help to identify the degree of activation (Castellano, Bosch-Queralt, Almolda, Villacampa, & Gonzalez, 2016; Hsieh et al., 2013; Perego, Fumagalli, & De Simoni, 2011). We used a CD68 marker to identify activated MG/Mϕ, with a preference for phagocytic cells (Perego et al., 2011). We found a significant elevation in CD68 cells by 1 dpi in male mice, which continued to increase through 7 dpi. In female mice we did not see significant increases in CD68 positive cells until 7 dpi, again demonstrating that female MG/Mϕ have a blunted response to TBI compared with male MG/Mϕ.

P2Y12 has been identified as a receptor that distinguishes CNS-resident ramified microglia from other blood-derived myeloid lineage cells (Butovsky et al., 2014; Kumar et al., 2016b; Moore et al., 2015), and loss of P2Y12 expression in microglia results in a decreased number of processes and cell migration following focal injury (Haynes et al., 2006). We found a dense population of microglial cells expressing P2Y12 marker in sham brains that remained after injury in both sexes. P2Y12 expression in microglial cells has been reported to diminish as the microglial cells become fully activated (Haynes et al., 2006), however, we clearly observed ramified and activated P2Y12-positive microglial cells up to 7 dpi in both male and female mice. Previous reports also demonstrate that P2Y12 is preferentially expressed in CD68+/CD163+ (anti-inflammatory) MG/Mϕ during parasitic brain infection (Moore et al., 2015), however in our study we did not observe any evidence that P2Y12 positive cells were better associated with specific cytokines after brain injury.

Rapid infiltration of peripheral cells plays a critical role in mediating sex differences in the brain response to experimental stroke, with splenectomy prior to ischemia eliminating the sex differences in infarct volume and activated brain MG/Mϕ in mice (Dotson, Wang, Saugstad, Murphy, Offner, 2015). Similarly, TBI also triggers infiltration of circulating blood cells (Hsieh et al., 2013; Jin et al., 2012), and we used the presence of the F4/80 protein as an indicator of macrophage recruitment to the CNS, as has been previously described (Hsieh et al., 2013; Kumar et al., 2016b; Morganti, Jopson, Liu, Gupta, & Rosi, 2014). We

observed that male mice had a high expression of F4/80 positive cells by 1 dpi that were highly concentrated at the lesion border. Female TBI brain had very low levels of F4/80 positive MG/Mϕ until 7 dpi when these cells became apparent around the lesion border. Very few F4/80-positive cells overlapped with P2Y12-positive cells in mouse brain after injury indicating distinct populations. Our data are in agreement with findings from the ischemia field where male mice have more peripheral leukocytes 3 days after hypoxia-ischemia compared with females (Mirza, Ritzel, Xu, McCullough, & Liu, 2015), causing increased secondary neuronal damage. Together these data suggest that female mice have reduced peripheral inflammatory cell infiltration to the injured CNS, which appears to protect against acute neuronal injury.

Morphological changes have been associated with the grade of activation and production of specific cytokines (Cao, Thomas, Ziebell, Pauly, & Lifshitz, 2012; Tam & Ma, 2014), and the persistent production of inflammatory cytokines by microglia results in chronic neuroinflammation after TBI (Loane & Byrnes, 2010). To analyze the cytokine expression in MG/Mϕ cells following TBI, we used a novel *in situ* hybridization technique for labeling specific RNA sequences in brain slices, combined with immunofluorescence using a cocktail of antibodies to detect the entire MG/Mϕ population. We used FISH as the use of antibodies against specific cytokines can produce variable results that may be because of the detection limit of immunohistochemistry for low levels of cytokines. The use of FISH improves specificity and sensitivity when examining cytokine mRNAs in distinct cells confirmed by antibody co-immunolabeling, which allows us to identify the cellular source of cytokine production following TBI with greater confidence. Our data demonstrates that a mixed pattern of both pro-inflammatory and anti-inflammatory cytokine expression occurred in MG/Mϕ in the first week after TBI. In male mice, both pro-and anti-inflammatory cytokines appeared at the same time-points. This is consistent with previous reports that there is an overlapping expression of phenotypic markers in MG/Mϕ following experimental TBI in male mice (Kim et al., 2016; Kumar et al., 2016a; Morganti et al., 2016). IL1β and TNFα are two important pro-inflammatory cytokines produced after TBI (Kumar et al., 2016a) that are known to induce neuronal cell death. While MG/Mϕ cells were the primary source of TNFα mRNA, the IL1β mRNA signal was as much as 68% from nonmicroglial cells sources after TBI. There were clear differences in the male and female IL1β and TNFα cytokine mRNA expression levels. While male mice presented with a sustained cytokine peak between 1 and 7 dpi, there was an unexpected biphasic peak in pro-inflammatory cytokines that occurred at 4 h post-TBI in female mice that retreated and peaked again at 7 dpi. The mechanism and purpose of this biphasic peak are not known, but the reduced expression of IL1β and TNFα at 1 and 3 dpi in female mice may explain the acute differences in neuroprotection between sexes.

One of the best characterized alternative-activation markers is Arg1, which contributes to wound healing and matrix deposition, and outcompetes iNOS to downregulate production of nitric oxide (Bansal & Ochoa, 2003). We found a strong Arg1 signal at the lesion border at 3 and 7 dpi in males. This is consistent with previous reports that show a sustained increase of Arg1 up 7 days post-TBI, with most of the Arg1

positive MG/Mϕ being hypertrophic/amoeboid and located near the cortical lesion (Kumar et al., 2016a). However, in our study, only male mice showed this strong Arg1-positive signal at the lesion border. In fact, we only detected a significant increase in Arg1 cells in female mouse brain at 30 dpi. We also studied the expression of TGFβ which is thought to be an anti-inflammatory cytokine, but with chronic exposure can also induce pro-inflammatory responses (Cohen et al., 2014). Again, we report a sexual dimorphism in TGFβ mRNA at 1 dpi, but this is resolved by 3 dpi.

Multiple reports have noted that females rodents appear protected against the effects of CNS injury compared with males (Dang, Mitkari, Kipp, & Beyer, 2011; Fleiss, Nilsson, Blomgren, & Mallard, 2012; Igarashi, Huang, & Noble, 2001) but conversely a study examining the effect of sex on TBI outcome in mice report no effect on lesion volume (Bruce-Keller et al., 2007; Tucker, Burke, Fu, & McCabe, 2017; Tucker, Fu, & McCabe, 2016; Xiong et al., 2007). Most of these studies have examined a single time-point postinjury, but in the current study, we found that female mice had a faster resolution of TUNEL staining compared with male mice, which correlated with smaller lesion volume at 3 and 7 dpi. The increased expression of pro-inflammatory cytokines in male mice occurred in the acute phase and could explain why male mice have increased cell death and larger lesion volume. Lesion in male mice followed a classical pattern that has previously been reported (Villapol et al., 2014). However, this pattern did not occur in female mice. When we continued to study lesion size over time and report that by 30 dpi, we do not detect any difference in lesion volume between male and female mice. A limitation of our study is that our chronic outcome measures were restricted to histological lesion volume. We have previously shown that the moderate-to-severe CCI used in this study, can be difficult to distinguish from severe CCI when using lesion volume alone (Washington et al., 2012). Other groups have used in-depth behavioral studies to study sex-differences after preclinical TBI. Similar to our findings, Tucker et al. demonstrated that female mice had a similar lesion volume to male mice 30 days after CCI, and presented with similar behavioral deficits in the Morris Water maze and rotarod test, although female mice display fewer anxiety-like behaviors after CCI (Tucker et al., 2016, 2017). Other studies have found that female rats have better motor function following TBI compared with males (Roof, Duvdevani, & Stein, 1993; Wagner et al., 2004). These confounding data may be explained by a study where the motor and cognitive function were assessed alongside lesion volume in male and female TBI mice. The authors found no difference in lesion volume or cognitive ability, but still report a significant reduction in foot-faults in female mice after TBI (Xiong et al., 2007). More studies are required to establish whether the differences in acute inflammatory responses can be harnessed to improve outcome in female mice after TBI.

A second limitation of our study is that we did not monitor the estrous cycle of our mice at the time of injury. We used random cycling in our mice to better resemble the clinical setting of TBI in cycling females. Previous studies have revealed that the estrous cycle stage at the time of the injury has no effect on postinjury neuroprotection of female mice and rats (Bramlett & Dietrich, 2001; Monaco et al., 2013).

In addition, when TBI was induced at random stages of the estrous cycle the performance variability was similar to that reported in male mice (Tucker et al., 2016, 2017).

In summary, in this work, we have demonstrated that female mice are acutely more resistant to moderate-to-severe TBI compared with male mice, primarily because of reduced neuroinflammation. However, this may not result in neuroprotection as female and male mice have similar brain volume loss at 30d post-TBI. It is clear that further research aimed at investigating the effects of sex, microglial function, and cell death are needed to elucidate the molecular and cellular mechanisms underlying hormonal and sex-related differences in the incidence and clinical course of brain injuries. Future studies will be essential for exploring personalized therapeutic treatments for TBI patients of both sexes.

ACKNOWLEDGMENTS

REFERENCES

Acaz-Fonseca, E., Duran, J. C., Carrero, P., Garcia-Segura, L. M., & Arevalo, M. A. (2015). Sex differences in glia reactivity after cortical brain injury. *Glia 63*, 1966–1981.

Arevalo, M. A., Santos-Galindo, M., Acaz-Fonseca, E., Azcoitia, I., & Garcia-Segura, L. M. (2013). Gonadal hormones and the control of reactive gliosis. *Hormones and Behavior 63*, 216–221.

Ayoub, A. E., & Salm, A. K. (2003). Increased morphological diversity of microglia in the activated hypothalamic supraoptic nucleus. *Journal of Neuroscience 23*, 7759–7766.

Bansal, V., & Ochoa, J. B. (2003). Arginine availability, arginase, and the immune response. *Current Opinion in Clinical Nutrition & Metabolic Care 6*, 223–228.

Belcredito, S., Vegeto, E., Brusadelli, A., Ghisletti, S., Mussi, P., Ciana, P., & Maggi, A. (2001). Estrogen neuroprotection: The involvement of the Bcl-2 binding protein BNIP2. *Brain Research Reviews 37*, 335–342.

Bramlett, H. M., & Dietrich, W. D. (2001). Neuropathological protection after traumatic brain injury in intact female rats versus males or ovariectomized females. *Journal of Neurotrauma 18*, 891–900.

Bruce-Keller, A. J., Dimayuga, F. O., Reed, J. L., Wang, C., Angers, R., ... Scheff, S. W. (2007). Gender and estrogen manipulation do not affect traumatic brain injury in mice. *Journal of Neurotrauma 24*, 203–215.

Bruce-Keller, A. J., Keeling, J. L., Keller, J. N., Huang, F. F., Camondola, S., & Mattson, M. P. (2000). Antiinflammatory effects of estrogen on microglial activation. *Endocrinology 141*, 3646–3656.

Butovsky, O., Jedrychowski, M. P., Moore, C. S., Cialic, R., Lanser, A. J., Gabriely, G., ... Weiner, H. L. (2014). Identification of a unique TGF-beta-dependent molecular and functional signature in microglia. *Nature Neuroscience 17*, 131–143.

Cao, T., Thomas, T. C., Ziebell, J. M., Pauly, J. R., & Lifshitz, J. (2012). Morphological and genetic activation of microglia after diffuse traumatic brain injury in the rat. *Neuroscience 225*, 65–75.

Caplan, H. W., Cox, C. S., & Bedi, S. S. (2017). Do microglia play a role in sex differences in TBI?. *Journal of Neuroscience Research 95*, 509–517.

Castellano, B., Bosch-Queralt, M., Almolda, B., Villacampa, N., & Gonzalez, B. (2016). Purine signaling and microglial wrapping. *Advances in Experimental Medicine and Biology 949*, 147–165.

Choi, S., & Friedman, W. J. (2009). Inflammatory cytokines IL-1beta and TNF-alpha regulate p75NTR expression in CNS neurons and astrocytes by distinct cell-type-specific signalling mechanisms. *ASN Neuro 1*,

Cohen, M., Matcovitch, O., David, E., Barnett-Itzhaki, Z., Keren-Shaul, H., Blecher-Gonen, R., . . . Schwartz, M. (2014). Chronic exposure to TGFbeta1 regulates myeloid cell inflammatory response in an IRF7-dependent manner. *embo Journal 33*, 2906–2921.

Corps, K. N., Roth, T. L., & McGavern, D. B. (2015). Inflammation and neuroprotection in traumatic brain injury. *JAMA Neurology 72*, 355–362.

Crain, J. M., Nikodemova, M., & Watters, J. J. (2013). Microglia express distinct M1 and M2 phenotypic markers in the postnatal and adult central nervous system in male and female mice. *Journal of Neuroscience Research 91*, 1143–1151.

Dang, J., Mitkari, B., Kipp, M., & Beyer, C(2011). Gonadal steroids prevent cell damage and stimulate behavioral recovery after transient middle cerebral artery occlusion in male and female rats. *Brain, Behaviour, and Immunity 25*, 715–726.

Dimayuga, F. O., Reed, J. L., Carnero, G. A., Wang, C., Dimayuga, E. R., Dimayuga, V. M., . . . Bruce-Keller, A. J. (2005). Estrogen and brain inflammation: Effects on microglial expression of MHC, costimulatory molecules and cytokines. *Journal of Neuroimmunology 161*, 123–136.

Dotson, A. L., Wang, J., Saugstad, J., Murphy, S. J., & Offner, H. (2015). Splenectomy reduces infarct volume and neuroinflammation in male but not female mice in experimental stroke. *Journal of Neuroimmunology 278*, 289–298.

Doyle, H. H., Eidson, L. N., Sinkiewicz, D. M., & Murphy, A. Z. (2017). Sex differences in microglia activity within the periaqueductal gray of the rat: A potential mechanism driving the dimorphic effects of morphine. *Journal of Neuroscience 37*, 3202–3214.

Durafourt, B. A., Moore, C. S., Zammit, D. A., Johnson, T. A., Zaguia, F., Guiot, M. C, . . . Antel, J. P. (2012). Comparison of polarization properties of human adult microglia and blood-derived macrophages. *Glia 60*, 717–727.

Engler-Chiurazzi, E. B., Brown, C. M., Povroznik, J. M., & Simpkins, J. W. (2016). Estrogens as neuroprotectants, Estrogenic actions in the context of cognitive aging and brain injury. *Progress in Neurobiology*, in press

Faden, A. I., Wu, J., Stoica, B. A., & Loane, D. J. (2016). Progressive inflammation-mediated neurodegeneration after traumatic brain or spinal cord injury. *British Journal of Pharmacology 173*:681–691.

Fleiss, B., Nilsson, M. K., Blomgren, K., & Mallard, C. (2012). Neuroprotection by the histone deacetylase inhibitor trichostatin A in a model of lipopolysaccharide-sensitised neonatal hypoxic-ischaemic brain injury. *Journal of Neuroinflammation 9*, 70-

Glenn, J. A, Ward, S. A., Stone, C. R., Booth, P. L., & Thomas, W. E. (1992). Characterisation of ramified microglial cells: Detailed morphology, morphological plasticity and proliferative capability. *Journal of Anatomy 180*, 109–118.

Goodman, Y., Bruce, A. J., Cheng, B., & Mattson, M. P. (1996). Estrogens attenuate and corticosterone exacerbates excitotoxicity, oxidative injury, and amyloid beta-peptide toxicity in hippocampal neurons. *Journal of Neurochemistry 66*, 1836–1844.

Habib, P., & Beyer, C. (2015). Regulation of brain microglia by female gonadal steroids. *Journal of Steroid Biochemistry and Molecular Biology 146*, 3–14.

Harry, G. J., & Kraft, A. D. (2008). Neuroinflammation and microglia: Considerations and approaches for neurotoxicity assessment. *Expert Opinion on Drug Metabolism & Toxicology 4*, 1265–1277.

Haynes, S. E., Hollopeter, G., Yang, G., Kurpius, D., Dailey, M. E., . . .Julius, D. (2006). The P2Y12 receptor regulates microglial activation by extracellular nucleotides. *Nature Neuroscience 9*, 1512–1519.

Hsieh, C. L., Kim, C. C., Ryba, B. E., Niemi, E. C., Bando, J. K., Locksley, R. M., . . . Seaman, W. E. (2013). Traumatic brain injury induces macrophage subsets in the brain. *Eur Journal of Immunology 43*, 2010–2022.

Igarashi, T., Huang, T. T., & Noble, L. J.. (2001). Regional vulnerability after traumatic brain injury: Gender differences in mice that overexpress human copper, zinc superoxide dismutase. *Experimetal Neurology 172*, 332–341.

Jin, X., Ishii, H., Bai, Z., Itokazu, T., & Yamashita, T. (2012). Temporal changes in cell marker expression and cellular infiltration in a controlled cortical impact model in adult male C57BL/6 mice. *PLoS One 7*, e41892-

Johnson, V. E., Stewart, J. E., Begbie, F. D., Trojanowski, J. Q., Smith, D. H., & Stewart, W. (2013). Inflammation and white matter degeneration persist for years after a single traumatic brain injury. *Brain 136*, 28–42.

Kettenmann, H., Hanisch, U. K., Noda, M., & Verkhratsky, A. (2011). Physiology of microglia. *Physiological Reviews 91*, 461–553.

Kim, C. C., Nakamura, M. C., & Hsieh, C. L. (2016). Brain trauma elicits non-canonical macrophage activation states. *Journal of Neuroinflammation 13*, 117-

Kumar, A., Alvarez-Croda, D. M., Stoica, B. A., Faden, A. I., & Loane, D. J. (2016a). Microglial/Macrophage Polarization Dynamics following Traumatic Brain Injury. *Journal of Neurotrauma 33*, 1732–1750.

Kumar, A., Barrett, J. P., Alvarez-Croda, D. M., Stoica, B. A., Faden, A. I., & Loane, D. J. (2016b). NOX2 drives M1-like microglial/macrophage activation and neurodegeneration following experimental traumatic brain injury. *Brain, Behaviour, and Immunity 58*, 291–309

Kumar, A., Stoica, B. A., Sabirzhanov, B., Burns, M. P., Faden, A. I., & Loane, D. J. (2013). Traumatic brain injury in aged animals increases lesion size and chronically alters microglial/macrophage classical and alternative activation states. *Neurobiology of Aging 34*, 1397–1411.

Loane, D. J., & Byrnes, K. R. (2010). Role of microglia in neurotrauma. *Neurotherapeutics 7*, 366–377.

Loane, D. J., Kumar, A., Stoica, B. A., Cabatbat, R., & Faden, A. I. (2014). Progressive neurodegeneration after experimental brain trauma: association with chronic microglial activation. *J Neuropathol Exp Neurol. 73*, 14–29.

Martinez, F. O., & Gordon, S. (2014). The M1 and M2 paradigm of macrophage activation: Time for reassessment. *F1000Prime Reports 6*, 13-

McCullough, L. D., de Vries, G. J., Miller, V. M., Becker, J. B., Sandberg, K., & McCarthy, M. M. (2014). NIH initiative to balance sex of animals in preclinical studies: Generative questions to guide policy, implementation, and metrics. *Biology of Sex Differences 5*, 15–

Mirza, M. A., Ritzel, R., Xu, Y., McCullough, L. D., & Liu, F. (2015). Sexually dimorphic outcomes and inflammatory responses in hypoxic-ischemic encephalopathy. *Journal of Neuroinflammation 12*, 32-

Mishra, S. K., Kumar, B. S., Khushu, S., Singh, A. K., & Gangenahalli, G.. (2016). Early monitoring and quantitative evaluation of macrophage infiltration after experimental traumatic brain injury: A magnetic resonance imaging and flow cytometric analysis. *Molecular and Cellular Neuroscience 78*, 25–34.

Monaco, C. M., Mattiola, V. V., Folweiler, K. A., Tay, J. K., Yelleswarapu, N. K., Curatolo, L. M., ... Kline, A. E. (2013). Environmental enrichment promotes robust functional and histological benefits in female rats after controlled cortical impact injury. *Experimetal Neurology 247*, 410–418.

Moore, C. S., Ase, A. R., Kinsara, A., Rao, V. T., Michell-Robinson, M., Leong, S. Y., ... Antel, J. P. (2015). P2Y12 expression and function in alternatively activated human microglia. *Neurology: Neuroimmunology and Neuroinflammation 2*, e80-

Morganti, J. M., Jopson, T. D., Liu, S., Gupta, N., & Rosi, S. (2014). Cranial irradiation alters the brain's microenvironment and permits CCR2+ macrophage infiltration. *PLoS One 9*, e93650-

Morganti, J. M., Jopson, T. D., Liu, S., Riparip, L. K., Guandique, C. K., Gupta, N., ... Rosi, S. (2015). CCR2 antagonism alters brain macrophage polarization and ameliorates cognitive dysfunction induced by traumatic brain injury. *Journal of Neuroscience 35*, 748–760.

Morganti, J. M., Riparip, L. K., & Rosi, S. (2016). Call Off the Dog(ma): M1/M2 Polarization Is Concurrent following Traumatic Brain Injury. *PLoS One 11*, e0148001-

Nimmerjahn, A., Kirchhoff, F., & Helmchen, F. (2005). Resting microglial cells are highly dynamic surveillants of brain parenchyma in vivo. *Science 308*, 1314–1318.

Ohsawa, K., Irino, Y., Sanagi, T., Nakamura, Y., Suzuki, E., Inoue, K., & Kohsaka, S. (2010). P2Y12 receptor-mediated integrin-beta1 activation regulates microglial process extension induced by ATP. *Glia 58*, 790–801.

Ohsawa, K., & Kohsaka, S. (2011). Dynamic motility of microglia: Purinergic modulation of microglial movement in the normal and pathological brain. *Glia 59*, 1793–1799.

Orihuela, R., McPherson, C. A., & Harry, G. J. (2016). Microglial M1/M2 polarization and metabolic states. *British Journal of Pharmacology 173*, 649–665.

Perego, C., Fumagalli, S., & De Simoni, M. G. (2011). Temporal pattern of expression and colocalization of microglia/macrophage phenotype markers following brain ischemic injury in mice. *Journal of Neuroinflammation 8*, 174-

Ransohoff, R. M., & Perry, V. H. (2009). Microglial physiology: Unique stimuli, specialized responses. *Annual Review of Immunology 27*, 119–145.

Rice, R. A., Pham, J., Lee, R. J., Najafi, A. R., West, B. L., & Green, K. N. (2017). Microglial repopulation resolves inflammation and promotes brain recovery after injury. *Glia 65*, 931–944.

Roof, R. L., Duvdevani, R., & Stein, D. G.. (1993). Gender influences outcome of brain injury: Progesterone plays a protective role. *Brain Research 607*, 333–336.

Saijo, K., & Glass, C. K. (2011). Microglial cell origin and phenotypes in health and disease. *Natures Review Immunology 11*, 775–787.

Sawada, M., Alkayed, N. J., Goto, S., Crain, B. J., Traystman, R. J., Shaivitz, A., Nelson, R. J., & Hurn, P. D. (2000). Estrogen receptor antagonist ICI182,780 exacerbates ischemic injury in female mouse. *Journal of Cerebral Blood Flow and Metabolism 20*, 112–118.

Schnell, L., Fearn, S., Klassen, H., Schwab, M. E., & Perry, V. H. (1999). Acute inflammatory responses to mechanical lesions in the CNS: Differences between brain and spinal cord. *European Journal of Neuroscience 11*, 3648–3658.

Selenica, M. L., Alvarez, J. A., Nash, K. R., Lee, D. C., Cao, C., Lin, X., ... Gordon, M. N. (2013). Diverse activation of microglia by chemokine (C-C motif) ligand 2 overexpression in brain. *Journal of Neuroinflammation 10*, 86-

Smith, C., Gentleman, S. M., Leclercq, P. D., Murray, L. S., Griffin, W. S., Graham, D. I., & Nicoll, J. A. (2013). The neuroinflammatory response in humans after traumatic brain injury. *Neuropathology Appl Neurobiology 39*, 654–666.

Srinivasan, D., Yen, J. H., Joseph, D. J., & Friedman, W. (2004). Cell type-specific interleukin-1beta signaling in the CNS. *Journal of Neuroscience 24*, 6482–6488.

Stein, D. G.. (2015). Embracing failure: What the Phase III progesterone studies can teach about TBI clinical trials. *Brain Injury 29*, 1259–1272.

Stence, N., Waite, M., & Dailey, M. E. (2001). Dynamics of microglial activation: A confocal time-lapse analysis in hippocampal slices. *Glia 33*, 256–266.

Tam, W. Y., & Ma, C. H. (2014). Bipolar/rod-shaped microglia are proliferating microglia with distinct M1/M2 phenotypes. *Scientific Report 4*, 7279-

Tang, Y., & Le, W. (2016). Differential Roles of M1 and M2 Microglia in Neurodegenerative Diseases. *Molecular Neurobiology 53*, 1181–1194.

Tucker, L. B., Burke, J. F., Fu, A. H., & McCabe, J. T. (2017). Neuropsychiatric symptom modeling in male and female C57BL/6J mice after experimental traumatic brain injury. *Journal of Neurotrauma 34*, 890–905.

Tucker, L. B., Fu, A. H., & McCabe, J. T. (2016). Performance of male and female C57BL/6J mice on motor and cognitive tasks commonly used in pre-clinical traumatic brain injury research. *Journal of Neurotrauma 33*, 880–894.

Vegeto, E., Bonincontro, C., Pollio, G., Sala, A., Viappiani, S., Nardi, F., ... Maggi, A. (2001). Estrogen prevents the lipopolysaccharide-induced inflammatory response in microglia. *Journal of Neuroscience 21*, 1809–1818.

Villapol, S., Balarezo, M. G., Affram, K., Saavedra, J. M., & Symes, A. J. (2015). Neurorestoration after traumatic brain injury through angiotensin II receptor blockage. *Brain 138*, 3299–3315.

Villapol, S., Byrnes, K. R., & Symes, A. J.. (2014). Temporal dynamics of cerebral blood flow, cortical damage, apoptosis, astrocyte-vasculature interaction and astrogliosis in the pericontusional region after traumatic brain injury. *Frontiers in Neurology 5*, 82-

Villapol, S., Wang, Y., Adams, M., & Symes, A. J. (2013). Smad3 deficiency increases cortical and hippocampal neuronal loss following traumatic brain injury. *Experimental Neurology 250*, 353–365.

Villapol, S., Yaszemski, A. K., Logan, T. T., Sanchez-Lemus, E., Saavedra, J. M., & Symes, A. J. (2012). Candesartan, an angiotensin II AT(1)-receptor blocker and PPAR-gamma agonist, reduces lesion volume and improves motor and memory function after traumatic brain injury in mice. *Neuropsychopharmacology 37*, 2817–2829.

Wagner, A. K., Willard, L. A., Kline, A. E., Wenger, M. K., Bolinger, B. D., Ren, D., ... Dixon, C. E. (2004). Evaluation of estrous cycle stage and gender on behavioral outcome after experimental traumatic brain injury. *Brain Research 998*, 113–121.

Washington, P. M., Forcelli, P. A., Wilkins, T., Zapple, D. N., Parsadanian, M., & Burns, M. P. (2012). The effect of injury severity on behavior: A phenotypic study of cognitive and emotional deficits after mild, moderate, and severe controlled cortical impact injury in mice. *Journal of Neurotrauma 29*, 2283–2296.

Xiong, Y., Mahmood, A., Lu, D., Qu, C., Goussev, A., Schallert, T., & Chopp, M. (2007). Role of gender in outcome after traumatic brain injury and therapeutic effect of erythropoietin in mice. *Brain Research 1185*, 301–312.